

# Naphthodithiophenediimide (NDTI): Synthesis, Structure, and Applications

Yuta Fukutomi,<sup>†,‡</sup> Masahiro Nakano,<sup>§,†,‡</sup> Jian-Yong Hu,<sup>§</sup> Itaru Osaka,<sup>§,†</sup> and Kazuo Takimiya<sup>\*,§,†</sup>

<sup>§</sup>Emergent Molecular Function Research Group, RIKEN Center for Emergent Matter Science (CEMS), Wako, Saitama 351-0198, Japan

<sup>†</sup>Department of Applied Chemistry, Graduate School of Engineering, Hiroshima University, Higashi-Hiroshima 739-8527, Japan

**S** Supporting Information

**ABSTRACT:** A straightforward synthesis of  $\alpha,\beta$ -unsubstituted and  $\alpha$ -halogenated naphtho[2,3-*b*:6,7-*b'*]-dithiophenediimides (NDTIs) is described. Electrochemical and optical studies of *N,N*-dioctyl-NDTI demonstrate that the compound has a low-lying LUMO energy level (4.0 eV below the vacuum level) and a small HOMO–LUMO gap ( $\sim 2.1$  eV). With its interesting electronic and optical properties, in addition to its planar structure, NDTI is a promising building block for the development of novel  $\pi$ -functional materials. In fact, it afforded n-channel, p-channel, and ambipolar materials, depending on the molecular modification.

1,4,5,8-Naphthalenediimide (NDI) is a well-known prototypical  $\pi$ -core that has found use as a chromophore, an electronic material, and a supramolecular architecture.<sup>1</sup> The molecular modification of NDI to yield core-substituted NDIs (cNDIs) has afforded a variety of materials for use as dyes, pigments, sensors, aggregates, and n- and p-type organic semiconductors.<sup>2</sup> A particularly important class of cNDIs for electronic applications is the  $\pi$ -extended cNDIs (Figure 1): core-linked NDIs, e.g., P(NDI2OD-T2), developed by Facchetti and co-workers have enabled the first high-mobility ( $\sim 1.0$  cm<sup>2</sup> V<sup>-1</sup> s<sup>-1</sup>) electron transport in polymer-based thin film transistors.<sup>3</sup> On the other hand, a recently emerging material class is the core-extended NDIs, where the NDI core and the other  $\pi$ -units are combined in a fused manner (Figure 1). This can afford rigid  $\pi$ -

frameworks with distinct electronic structures from relatively simple core-linked NDIs. A prominent example of the core-extended NDIs is the (1,3-dithiol-2-ylidene)malononitrile-fused derivative (NDI-DTYM) reported by Zhu et al., which has enabled the production of solution-processed n-channel OFETs having extraordinarily high electron mobility of up to 3.5 cm<sup>2</sup> V<sup>-1</sup> s<sup>-1</sup> and stability in ambient conditions.<sup>4</sup> In addition, various aromatic<sup>5</sup> and heteroaromatic-fused NDIs, including thiophene,<sup>4b,6</sup> pyrrole,<sup>7</sup> pyrazine,<sup>8</sup> and thiazole-fused<sup>9</sup> derivatives, were recently developed as promising candidates for optoelectronic materials.

Among such heteroaromatic-fused NDIs, thiophene-fused NDIs, 4,5,9,10-naphtho[2,3-*b*:6,7-*b'*]dithiophenediimides (NDTIs, Scheme 1), in particular, ones with  $\alpha$ - and  $\beta$ -unsubstituted thiophenes are an attractive archetypical structure for the development of functional  $\pi$ -conjugated materials for the following reasons: (i) a planar and rigid structure over the whole  $\pi$ -framework, which is beneficial for carrier transport, owing to the small reorganization energies (Table S1)<sup>10</sup> and the favorable intermolecular  $\pi$ – $\pi$  overlap in the solid state; (ii) modification at vacant thiophene  $\alpha$ -positions in the NDTI core which enables further  $\pi$ -extension and incorporation into the backbone structures in conjugated oligomers and polymers while maintaining good coplanarity leading to various cNDIs. Although a tetracyano-substituted NDTI derivative was reported,<sup>4b</sup> to the best of our knowledge,  $\alpha,\beta$ -unsubstituted NDTIs have remained unknown.<sup>11</sup> Herein, we first describe a straightforward synthesis of NDTI and then discuss its molecular structure, electronic properties, and application to n-channel OFETs. We also demonstrate that  $\alpha$ -dihalogenated NDIs can be synthesized and utilized in the synthesis of conjugated polymers with the NDTI core in the polymer backbone.

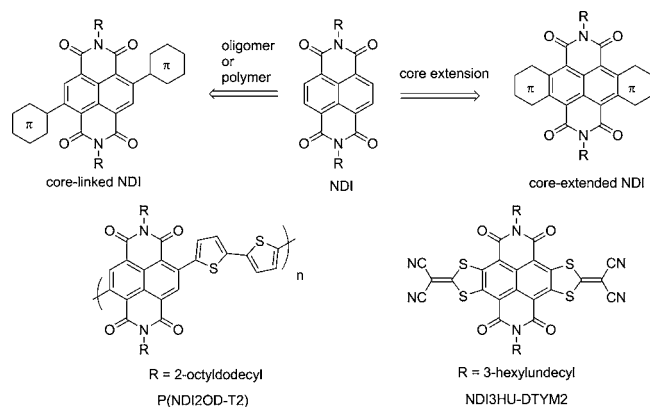
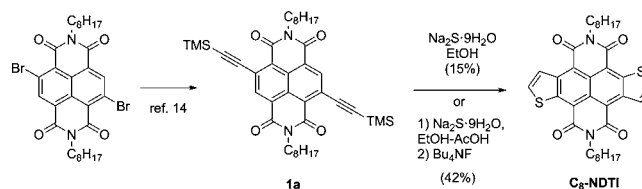


Figure 1.  $\pi$ -Extended cNDIs.

## Scheme 1. Synthesis of C<sub>8</sub>-NDTI



Received: May 12, 2013

Published: July 24, 2013

There may be several potential synthetic routes to the NDTI core, including ones from naphtho[2,3-*b*:6,7-*b'*]dithiophene (*anti*-NDTI)<sup>12</sup> or NDI derivatives. After many synthetic attempts, we finally found that a route from *N,N'*-dioctyl-2,6-dibromo-NDI ( $\text{Br}_2\text{NDI}$ )<sup>13</sup> is very effective (Scheme 1):  $\text{Br}_2\text{NDI}$  was readily converted into the corresponding bis-(trimethylsilyl)ethynyl intermediate (**1a**),<sup>14</sup> treatment of which with sodium sulfide hydrate ( $\text{Na}_2\text{S}\cdot 9\text{H}_2\text{O}$ ) in ethanol surprisingly gave the desired compound, *N,N'*-dioctyl-NDTI ( $\text{C}_8\text{-NDTI}$ ), in 15% isolated yield as a purple crystalline solid. Note that this one-pot reaction must involve the initial addition of the sulfide anion to the ethyne moiety and a subsequent intramolecular oxidative thiophene formation reaction (see Scheme S1 for a plausible reaction pathway).<sup>15</sup> However, yields of  $\text{C}_8\text{-NDTI}$  were always <15% even though various reaction conditions with different sulfur sources, temperatures, and solvents were examined. After conducting intensive trials aimed at improving the yield (Table S1), we finally found that the addition of acetic acid ( $\sim 2$  vol %) enhanced the yield of the thiophene annulation reaction (>40%) and the major product in the reaction was 2,7-bis(trimethylsilyl)-substituted  $\text{C}_8\text{-NDTI}$  (**2a**), the TMS groups of which could be easily cleaved off to afford  $\text{C}_8\text{-NDTI}$  in 42% yield from **1**.

The structure of  $\text{C}_8\text{-NDTI}$  was fully characterized by spectroscopic analysis.  $^1\text{H}$  NMR measurements showing two sets of doublets assignable to the  $\text{H}_\alpha$  and  $\text{H}_\beta$  atoms of the thiophene moieties and  $^{13}\text{C}$  NMR measurements yielding seven aromatic and two carbonyl carbons clearly indicated that the fused thiophene rings were in *anti*-configuration (see Supporting Information [SI]). Single-crystal X-ray analysis also confirmed the structure (Figure S1). A noticeable feature in the molecular structure of  $\text{C}_8\text{-NDTI}$  is the high planarity of the NDTI core (Figure 2), which is strikingly different from isoelectronic tetracenediimides<sup>5</sup> and related benzo[*b*]thiophene-fused NDI,<sup>6</sup> where steric repulsion between the peri-hydrogen atoms or the peri-substituents and imide oxygen atoms causes a large distortion of the cores. The packing structure of  $\text{C}_8\text{-NDTI}$  can be best described by a one-dimensional columnar structure along the crystallographic *b*-axis with relatively close  $\pi$ -stacking ( $\sim 3.43$  Å) (Figure 2b). As the NDTI planes largely tilt against the *b*-axis by  $\sim 45^\circ$ , approximately half of the NDT part overlaps with the neighboring molecules.

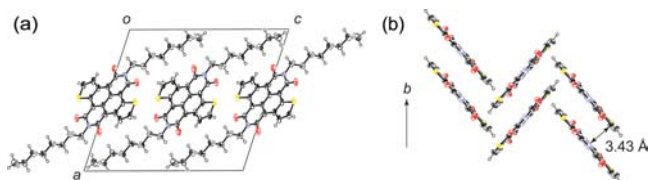


**Figure 2.** Packing structure of  $\text{C}_8\text{-NDTI}$ , viewed along the crystallographic *b*-axis direction (a) and side view of a  $\pi$ -stacking columnar structure (b); for clarity, octyl groups are omitted.

In Figure 3a are the cyclic voltammograms of  $\text{C}_8\text{-NDTI}$ ,  $\text{C}_8\text{-NDI}$ , and *anti*-NDTI.<sup>12</sup> From the reduction and oxidation potentials, the HOMO and LUMO energy levels ( $E_{\text{HOMO}}$  and  $E_{\text{LUMO}}$ ) of  $\text{C}_8\text{-NDTI}$  are estimated to be 6.1 and 4.0 eV, respectively, below the vacuum level. The  $E_{\text{LUMO}}$  of  $\text{C}_8\text{-NDTI}$  is close to that of  $\text{C}_8\text{-NDI}$  ( $-3.9$  eV), indicating that the LUMO is rather NDI-like and stabilized slightly by the lateral  $\pi$ -extension with thiophenes. In fact, the calculated  $E_{\text{LUMO}}$ 's as

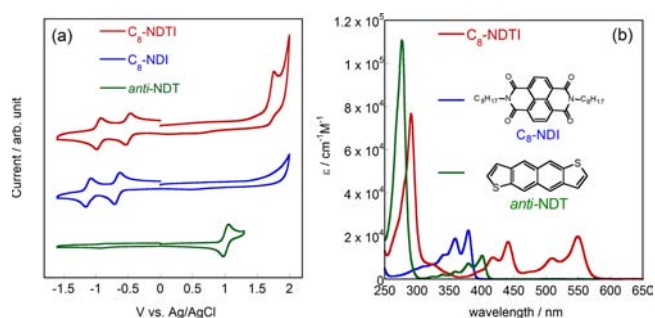


**Figure 3.** Cyclic voltammograms (a) and UV-vis absorption spectra in dichloromethane (b) of  $\text{C}_8\text{-NDTI}$  (red trace) together with  $\text{C}_8\text{-NDI}$  (blue trace) and *anti*-NDTI (green trace).

well as the LUMO geometries of the model compounds of  $\text{C}_8\text{-NDTI}$  and  $\text{C}_8\text{-NDI}$  are quite similar (Figure S2). On the other hand, the  $E_{\text{HOMO}}$  of  $\text{C}_8\text{-NDTI}$  lies in between those of *anti*-NDTI ( $-5.3$  eV) and  $\text{C}_8\text{-NDI}$  ( $-7.1$  eV, estimated from  $E_{\text{LUMO}}$  and the optical HOMO-LUMO gap). This can be understood from the calculated HOMO geometry of NDTI that can be qualitatively expressed as the superposition of those of *anti*-NDTI and NDI (Figure S2); both may contribute to the electronic structure of NDTI's HOMO, resulting in the  $E_{\text{HOMO}}$  lying in between these two. The electrochemical HOMO-LUMO gap ( $E_g$ ) of  $\text{C}_8\text{-NDTI}$  is  $\sim 2.1$  eV, consistent with the optical  $E_g$  (2.18 eV) estimated from the absorption onset ( $\sim 570$  nm) in the UV-vis absorption spectra of  $\text{C}_8\text{-NDTI}$  in solution (Figure 3b). The large bathochromic shift of  $\text{C}_8\text{-NDTI}$  compared with that of  $\text{C}_8\text{-NDI}$  is a common feature of the core-extended NDIs.<sup>5-9</sup> It is also interesting that  $\text{C}_8\text{-NDTI}$  showed intense fluorescence with high quantum efficiency ( $\Phi = 0.76$ ) (Figure S3), whereas almost no emission was observed for  $\text{C}_8\text{-NDI}$  solution under identical experimental conditions.<sup>16</sup>

As the low-lying  $E_{\text{LUMO}}$  of  $\text{C}_8\text{-NDTI}$  was similar to those of lateral-extended NDI derivatives, n-channel behavior was anticipated for its field-effect transistors (FETs).<sup>17</sup> The deposition of  $\text{C}_8\text{-NDTI}$  on substrates from solution gave poor-quality films consisting of many crystalline islands. This was probably due to its high crystallinity. On the other hand, vapor deposition of  $\text{C}_8\text{-NDTI}$  gave uniform thin films, and top-contact, bottom-gate OFETs fabricated with the vapor-deposited thin films showed typical n-channel transistor characteristics (Figure 4). Depending on the substrate surface treatment with hexamethyldisilazane (HMDS), octyltrichlorosilane (OTS), or octadecyltrichlorosilane (ODTS), and the

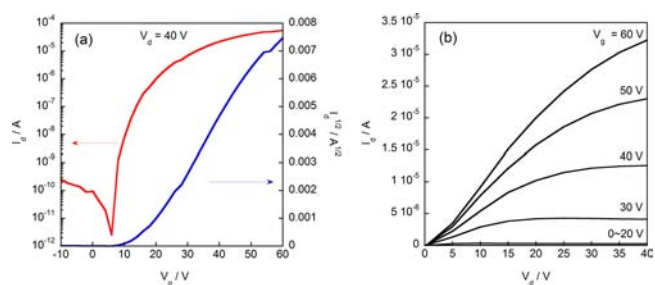


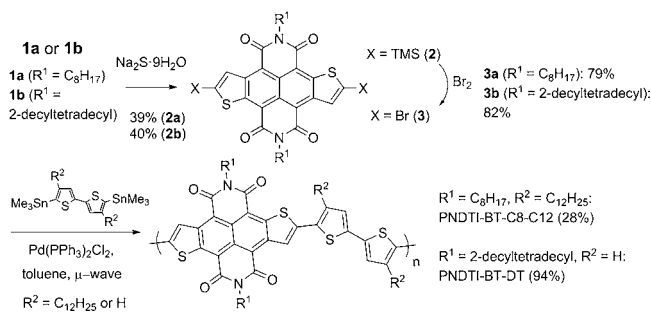
**Figure 4.** Transfer (a) and output (b) characteristics of  $\text{C}_8\text{-NDTI}$ -based OFET fabricated on OTS-midfield Si/SiO<sub>2</sub> substrate (SiO<sub>2</sub> thickness: 200 nm). The channel length and width are 40 and 3000  $\mu\text{m}$ , respectively. Electron mobilities were extracted from the saturation regime ( $V_d = V_g = 40$  V).

substrate temperature during film deposition ( $T_{\text{sub}}$ ), the electron mobility extracted from the saturation regime was somewhat varied (in the order of  $10^{-3}$  to  $10^{-2}$   $\text{cm}^2 \text{V}^{-1} \text{s}^{-1}$ , see Table S3). The best electron mobility evaluated under vacuum was  $0.05 \text{ cm}^2 \text{V}^{-1} \text{s}^{-1}$  on the ODTS-modified substrate at  $T_{\text{sub}} = 150 \text{ }^\circ\text{C}$ , which was only slightly reduced ( $\sim 0.02 \text{ cm}^2 \text{V}^{-1} \text{s}^{-1}$ ) under ambient conditions. The electron mobility of the present  $\text{C}_8$ -NDTI-based OFETs is comparable to those of related core-extended NDIs with aromatic/heteroaromatic rings so far reported: tetracenediimide:  $3.3 \times 10^{-3} \text{ cm}^2 \text{V}^{-1} \text{s}^{-1}$ ,<sup>5a</sup> indole-fused NDI:  $\sim 0.03 \text{ cm}^2 \text{V}^{-1} \text{s}^{-1}$ ,<sup>7</sup> and thiazole-fused NDIs:  $\sim 0.15 \text{ cm}^2 \text{V}^{-1} \text{s}^{-1}$ .<sup>9</sup>

The limited mobility of the  $\text{C}_8$ -NDTI-based OFETs can be related to the polymorphism of  $\text{C}_8$ -NDTI in the thin film state (Figure S4). The out-of-plane XRD pattern of the  $\text{C}_8$ -NDTI thin film clearly shows two series of peaks, one of which is assignable to a packing structure similar to that elucidated by single-crystal X-ray analysis, with the preferred orientation of the crystallographic  $a$ -axis along the normal to the substrate ( $d$ -spacing:  $16.6 \text{ \AA}$ , Figure 2a). Another series of peaks up to the sixth order with higher intensity corresponds to the  $d$ -spacing of  $19.7 \text{ \AA}$ , where the  $\text{C}_8$ -NDTI molecules are upright compared to the bulk single-crystal phase, implying favorable electron transport for the latter phase. At present, the improvement of thin film morphology by optimizing the deposition conditions is difficult, and thus, molecular modification is under way (see SI).

For the further utilization of the NDTI core in versatile functional  $\pi$ -systems via the lateral extension, the key chemistry is to introduce reactive functional groups at the thiophene  $\alpha$ -positions of NDTI. Starting from  $\text{C}_8$ -NDTI, therefore, various reactions, including electrophilic halogenation, Ir-catalyzed direct borylation,<sup>18</sup> and lithiation followed by electrophilic substitution, were attempted. However, all these failed, probably owing to the electron deficiency of the core and/or the low solubility of  $\text{C}_8$ -NDTI at low temperature. To overcome the inert nature of  $\text{C}_8$ -NDTI, we tested 2,7-bis(trimethylsilyl)-NDTI (**2a**) instead of  $\text{C}_8$ -NDTI for conversion into the corresponding bromide (Scheme 2). The conversion of **2a** by treatment with bromine gave corresponding dibromide (**3a**) in a good yield.<sup>19</sup> Then, **3a** was reacted with 5,5'-bis(trimethylstannyl)-3,3'-didodecyl-2,2'-bithiophene in the presence of palladium catalyst to give the corresponding polymer (PNDTI-BT-C8-C12) as a greenish black solid. After the usual workup, Soxhlet extraction with *o*-dichlorobenzene gave a polymer fraction with  $M_n = 12,900$ ,  $M_w = 26,900$ , and  $\text{PDI} = 2.1$  (28% isolated yield based on **3a**), although an insoluble solid remained in the extraction thimble, which

### Scheme 2. Synthesis of Brominated-NDTIs (**3**) and Utilization of **3** for the Synthesis of PNDTI-BT Copolymers



strongly implied that the limited solubility of PNDTI-BT-C8-C12 reduced the yield. To improve the solubility of the NDTI-based polymer, 2-decyltetradecyl groups were introduced into the NDTI core (Scheme 2) and the resulting polymer (PNDTI-BT-DT,  $M_n = 27,100$ ,  $M_w = 90,400$ , and  $\text{PDI} = 3.3$ ) was found to be soluble in chloroform at room temperature even without the addition of alkyl groups on the bithiophene comonomer unit. The yield was also improved significantly (94% after usual workup).

The evaluation of PNDTI-BTs was carried out using spin-coated films on quartz glass or Si/SiO<sub>2</sub> substrate from hot *o*-dichlorobenzene (PNDTI-BT-C8-C12) or chloroform solution (PNDTI-BT-DT). The absorption spectra of the thin films showed a large band centered at  $\sim 800 \text{ nm}$  with the absorption tail reaching  $\sim 1000 \text{ nm}$  (Figure 5a), indicating that the optical  $E_g$ 's are  $\sim 1.2 \text{ eV}$  for both polymers, which is comparable to that of related NDI-bithiophene copolymer, P(NDI2OD-T2).<sup>3</sup>  $E_{\text{HOMO}}$ 's of the polymers were determined to be  $-5.4 \text{ eV}$  (PNDTI-BT-C8-C12) and  $-5.6 \text{ eV}$  (PNDTI-BT-DT), respectively, by photoelectron spectroscopy in air (PESA, Figure S6), and estimated  $E_{\text{LUMO}}$ 's were  $-4.2$  and  $-4.4 \text{ eV}$ , respectively (Figure 5b). The difference in  $E_{\text{HOMO}}$  and  $E_{\text{LUMO}}$  between the two polymers could be caused by the electron-donating dodecyl groups on the bithiophene comonomer unit.

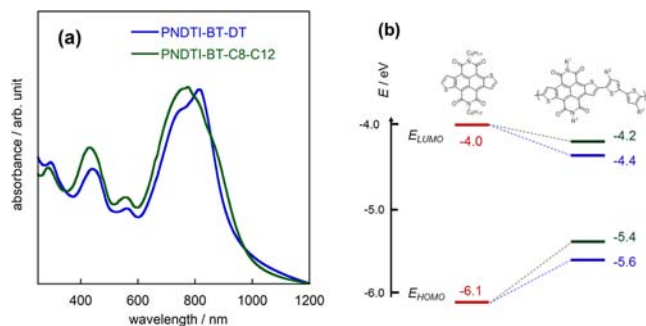


**Figure 5.** Absorption spectra (a) and estimated  $E_{\text{HOMO}}$  and  $E_{\text{LUMO}}$  (b) of PNDTI-BT-C8-C12 (green line) and PNDTI-BT-DT (blue line).

Most likely owing to the elevated  $E_{\text{HOMO}}$  of the polymers and the lateral  $\pi$ -extension that made the system quite favorable for p-channel conduction, as already pointed out by Würthner and co-workers,<sup>7</sup> the solution-processed OFETs showed hole transport with mobilities of up to  $4 \times 10^{-3}$  (PNDTI-BT-C8-C12, Figure S7) and  $0.10 \text{ cm}^2 \text{V}^{-1} \text{s}^{-1}$  (PNDTI-BT-DT, Figure 6a), respectively (Tables S4, 5). Although no obvious electron

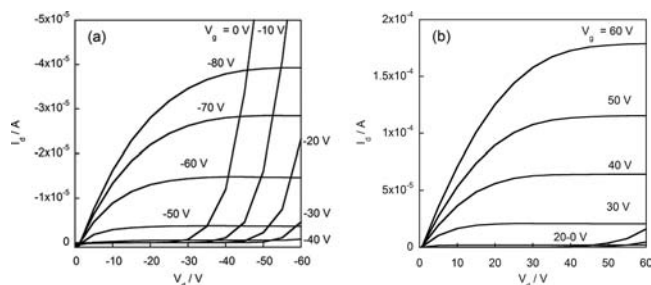


**Figure 6.** Output characteristics of PNDTI-BT-DT-based FET fabricated on ODTS-modified Si/SiO<sub>2</sub> substrate (SiO<sub>2</sub> thickness:  $200 \text{ nm}$ ): (a) p-channel operation, and (b) n-channel operation. Channel length =  $40 \text{ }\mu\text{m}$ ; width =  $3000 \text{ }\mu\text{m}$ .

transport was confirmed in the PNDTI-BT-C8-C12-based OFETs, the PNDTI-BT-DT-based OFETs also showed electron transport with mobility of  $0.27 \text{ cm}^2 \text{ V}^{-1} \text{ s}^{-1}$  (Figure 6b), indicating that the polymer has an ambipolar nature, similar to related NDI-based polymers.<sup>20</sup> The absence/presence of electron transport in the respective polymers could partially be related to the effects of the dodecyl groups on the bithiophene moiety: the electron-donating dodecyl groups raised  $E_{\text{HOMO}}$  and  $E_{\text{LUMO}}$  (Figure 5b), making PNDTI-BT-C8-C12 rather p-channel-favorable. These results reveal that the NDTI-based polymer system is a versatile semiconductor having a tunable charge type that is dependent on the incorporated comonomer unit.

In summary, we have established a reliable and straightforward access to  $\alpha,\beta$ -unsubstituted and  $\alpha$ -halogenated NDTIs. The characteristic features of NDTI are manifold: low-lying  $E_{\text{LUMO}}$ , elevation of  $E_{\text{HOMO}}$  by lateral  $\pi$ -extension, no *syn/anti*-isomerism, and a rigid and planar molecular structure with small reorganization energies for both electron and hole. All these features should be attractive for the development of new organic semiconductors. In fact, NDTI-based materials, depending on the chemical modification, can be used as n-channel, p-channel, or ambipolar semiconductors. Not only do they have potential applications to OFETs, they also show intriguing optical properties as well, e.g. strong fluorescence ( $C_8$ -NDTI) or a broad and intense absorption band in the near-infrared region (PNDTI-BTs) which make them useful for luminescent or photovoltaic devices,<sup>21</sup> respectively. As the present NDTI core has "chemical flexibility," i.e., both substituents on the imide nitrogen atoms and at the thiophene  $\alpha$ -positions can be modified, with the latter altering the electronic structure drastically, the NDTI core is a versatile and valuable building block for the development of new organic semiconductors in many aspects. We have high hopes that NDTI will contribute to the development of organic optoelectronic materials in the near future.

## ■ ASSOCIATED CONTENT

### Supporting Information

Experimental details and characterization data. This material is available free of charge via the Internet at <http://pubs.acs.org>.

## ■ AUTHOR INFORMATION

### Corresponding Author

takimiya@riken.jp

### Author Contributions

<sup>‡</sup>Y.F. and M.N. contributed to this paper equally.

### Notes

The authors declare no competing financial interest.

## ■ ACKNOWLEDGMENTS

This work was financially supported by Grants-in-Aid for Scientific Research (Nos. 23245041 and 24685030) from MEXT, Japan and The Strategic Promotion of Innovative Research and Development from the Japan Science and Technology Agency. HRMSs were carried out at the Natural Science Center for Basic Research and Development (N-BARD), Hiroshima University, and at the Materials Characterization Support Unit in RIKEN Advanced Technology Support Division. One of the authors (M.N.) is grateful for the research fellowship for young scientists from JSPS.

## ■ REFERENCES

- (1) (a) Vollmann, H.; Becker, H.; Corell, M.; Streeck, H. *Lieb. Ann.* **1937**, *531*, 1–159. (b) Bhosale, S. V.; Jani, C. H.; Langford, S. J. *Chem. Soc. Rev.* **2008**, *37*, 331–342. (c) Zhan, X.; Facchetti, A.; Barlow, S.; Marks, T. J.; Ratner, M. A.; Wasielewski, M. R.; Marder, S. R. *Adv. Mater.* **2011**, *23*, 268–284.
- (2) (a) Würthner, F.; Ahmed, S.; Thalacker, C.; Debaerdemaecker, T. *Chem.–Eur. J.* **2002**, *8*, 4742–4750. (b) Sakai, N.; Mareda, J.; Vauthey, E.; Matile, S. *Chem. Commun.* **2010**, *46*, 4225–4237. (c) Bhosale, S. V.; Bhosale, S. V.; Bhargava, S. K. *Org. Biomol. Chem.* **2012**, *10*, 6455–6468.
- (3) (a) Chen, Z.; Zheng, Y.; Yan, H.; Facchetti, A. *J. Am. Chem. Soc.* **2009**, *131*, 8–9. (b) Yan, H.; Chen, Z.; Zheng, Y.; Newman, C.; Quinn, J. R.; Dotz, F.; Kastler, M.; Facchetti, A. *Nature* **2009**, *457*, 679–686. (c) Hwang, Y.-J.; Murari, N. M.; Jenekhe, S. A. *Polym. Chem.* **2013**, *4*, 3187–3195.
- (4) (a) Gao, X.; Di, C.-a.; Hu, Y.; Yang, X.; Fan, H.; Zhang, F.; Liu, Y.; Li, H.; Zhu, D. *J. Am. Chem. Soc.* **2010**, *132*, 3697–3699. (b) Hu, Y.; Gao, X.; Di, C.-a.; Yang, X.; Zhang, F.; Liu, Y.; Li, H.; Zhu, D. *Chem. Mater.* **2011**, *23*, 1204–1215. (c) Hu, Y.; Qin, Y.; Gao, X.; Zhang, F.; Di, C.-a.; Zhao, Z.; Li, H.; Zhu, D. *Org. Lett.* **2012**, *14*, 292–295. (d) Zhang, F.; Hu, Y.; Schuettfort, T.; Di, C.-a.; Gao, X.; McNeill, C. R.; Thomsen, L.; Mannsfeld, S. C. B.; Yuan, W.; Sirringhaus, H.; Zhu, D. *J. Am. Chem. Soc.* **2013**, *135*, 2338–2349.
- (5) (a) Katsuta, S.; Tanaka, K.; Maruya, Y.; Mori, S.; Masuo, S.; Okujima, T.; Uno, H.; Nakayama, K.-i.; Yamada, H. *Chem. Commun.* **2011**, *47*, 10112–10114. (b) Yue, W.; Gao, J.; Li, Y.; Jiang, W.; Di Motta, S.; Negri, F.; Wang, Z. *J. Am. Chem. Soc.* **2011**, *133*, 18054–18057. (c) Yue, W.; Lv, A.; Gao, J.; Jiang, W.; Hao, L.; Li, C.; Li, Y.; Polander, L. E.; Barlow, S.; Hu, W.; Di Motta, S.; Negri, F.; Marder, S. R.; Wang, Z. *J. Am. Chem. Soc.* **2012**, *134*, 5770–5773. (d) Ye, Q.; Chang, J.; Huang, K.-W.; Chi, C. *Org. Lett.* **2011**, *13*, 5960–5963.
- (6) Gao, J.; Li, Y.; Wang, Z. *Org. Lett.* **2013**, *15*, 1366–1369.
- (7) Suraru, S.-L.; Zschieschang, U.; Klauk, H.; Würthner, F. *Chem. Commun.* **2011**, *47*, 11504–11506.
- (8) (a) Li, C.; Xiao, C.; Li, Y.; Wang, Z. *Org. Lett.* **2013**, *15*, 682–685. (b) Ye, Q.; Chang, J.; Huang, K.-W.; Shi, X.; Wu, J.; Chi, C. *Org. Lett.* **2013**, *15*, 1194–1197.
- (9) Chen, X.; Guo, Y.; Tan, L.; Yang, G.; Li, Y.; Zhang, G.; Liu, Z.; Xu, W.; Zhang, D. *J. Mater. Chem. C* **2013**, *1*, 1087–1092.
- (10) MO calculations were carried out with the DFT methods at the B3LYP/6-31g(d) level using Gaussian 03 program. See SI.
- (11) Related thiophene-fused coronene diimide was recently reported. See: Usta, H.; Newman, C.; Chen, Z.; Facchetti, A. *Adv. Mater.* **2012**, *24*, 3678–3684.
- (12) Shinamura, S.; Osaka, I.; Miyazaki, E.; Nakao, A.; Yamagishi, M.; Takeya, J.; Takimiya, K. *J. Am. Chem. Soc.* **2011**, *133*, 5024–5035.
- (13) Thalacker, C.; Röger, C.; Würthner, F. *J. Org. Chem.* **2006**, *71*, 8098–8105.
- (14) Buckland, D.; Bhosale, S. V.; Langford, S. J. *Tetrahedron Lett.* **2011**, *52*, 1990–1992.
- (15) Baranov, D. S.; Gold, B.; Vasilevsky, S. F.; Alabugin, I. V. *J. Org. Chem.* **2013**, *78*, 2074–2082.
- (16) Bullock, J. E.; Vagnini, M. T.; Ramanan, C.; Co, D. T.; Wilson, T. M.; Dicke, J. W.; Marks, T. J.; Wasielewski, M. R. *J. Phys. Chem. B* **2010**, *114*, 1794–1802.
- (17) (a) Katz, H. E.; Lovinger, A. J.; Johnson, J.; Kloc, C.; Siegrist, T.; Li, W.; Lin, Y. Y.; Dodabalapur, A. *Nature* **2000**, *404*, 478–481. (b) Würthner, F.; Stolte, M. *Chem. Commun.* **2011**, *47*, 5109–5115.
- (18) Mkhaldid, I. A. I.; Barnard, J. H.; Marder, T. B.; Murphy, J. M.; Hartwig, J. F. *Chem. Rev.* **2010**, *110*, 890–5931.
- (19) The corresponding iodide can also be prepared by reaction with iodine monochloride in a moderate yield. See SI.
- (20) (a) Baeg, K.-J.; Khim, D.; Jung, S.-W.; Kang, M.; You, I.-K.; Kim, D.-Y.; Facchetti, A.; Noh, Y.-Y. *Adv. Mater.* **2012**, *24*, 5433–5439. (b) Gu, C.; Hu, W.; Yao, J.; Fu, H. *Chem. Mater.* **2013**, *25*, 2178–2183.
- (21) Facchetti, A. *Mater. Today* **2013**, *16*, 123–132.